NASA TECHNICAL MEMORANDUM NASA TM-76530

PULL-OUT OF FIBERS FROM COMPOSITE MATERIALS AT HIGH RATE OF LOADING

S. Amijima and T. Fujii

Translation of article from:
Journal of Japan Society of Materials Science, vol. 28, Nov. 1979, p 1091-97.

NATIONAL AERONAUTICS AND SPACE ADMINISTRATION
WASHINGTON, DC 20546 MARCH 1981

STANDARD TITLE PAGE

1. Report No.	2. Government Accession No.	3. Recipient's Catalog No.
NASA TM-76530		

4. Title and Subtitle	5. Report Date
PULL-OUT OF FIBERS FROM COMPOSITE MATERIALS AT HIGH RATE OF LOADING	MARCH 1981
	6. Performing Organization Code

7. Author(s)	8. Performing Organization Report No.
S. Amijima and T. Fujii	10. Work Unit No.
	11. Contract or Grant No. NASw-3198

9. Performing Organization Name and Address	13. Type of Report and Period Covered
SCITRAN Box 5456 Santa Barbara, CA 93108	Translation
12. Sponsoring Agency Name and Address National Aeronautics and Space Administration Washington, D.C. 20546	14. Sponsoring Agency Code

15. Supplementary Notes Translation of article from:
Journal of Japan Society of Materials Science, vol. 28, Nov. 1979, p 1091-97. (A80-19909)

16. Abstract

Numerical and experimental results are presented on the pullout phenomenon in composite materials at a high rate of loading. The finite element method was used, taking into account the existence of a virtual shear deformation layer as the interface between fiber and matrix. Experimental results agree well with those obtained by the finite element method. Numerical results show that the interlaminar shear stress is time-dependent, in addition, it is shown to depend on the applied load-time history. Under step pulse loading, the interlaminar shear stress fluctuates, finally decaying to its value under static loading.

17. Key Words (Selected by Author(s))	18. Distribution Statement
	Unclassified - Unlimited

19. Security Classif. (of this report)	20. Security Classif. (of this page)	21. No. of Pages	22. Price
Unclassified	Unclassified	18	

PULL-OUT OF FIBERS FROM COMPOSITE MATERIALS AT HIGH RATE OF LOADING

S. Amijima# and T. Fujii##

1. Introduction

The pull-out phenomenon of fibers from a matrix is an important problem closely related to the stress transmission mechanism and fiber stripping processes in composite materials. This phenomenon is also a crucial factor of the impulsively absorbed energy, for example, obtained from impulse-tests on isots [1,2], as has been already pointed out by Outwater [3]. Lawrence investigated [4] the pull-out phenomenon of fibers from matrix layers under static loading. However, for a high rate of loading, it is often insufficient to rely only on the usual analysis of static loading. Namely, in static analysis shear stress waves propagating within a material have not been considered. Therefore, we investigated the pull-out phenomenon of fibers from composite materials at high rates of loading, numerically and experimentally, taking into account propagation of stress waves within materials and existence of a virtual shear deformation layer as an interface between a fiber and the matrix.

2. A pull-out model and equations of motion

Let us consider a one-dimensional model of Figure 1a to examine the pull-out phenomenon of fibers from fiber-enforced composite materials (or piled boards). In the model, two different layers are connected by a massless shear deformation layer (an adhesive layer). Through this shear layer propagates the shear stress that is proportional to relative displacement and inversely proportional to the layer thickness. The shear layer (the adhesive layer) in the model can be a matrix layer, or a kind of shear stress propagation layer (transition layer) at the interface between fibers and the matrix, if one considers

---

*Numbers in margin indicate pagination of foreign text.

Department of Mechanical Engineering, Doshisha University, Kyoto
Technical Research Development Institute, Japan Defense Agency, Saga- 1 mihara

Material 2 as a matrix. In the one-dimensional model, Figure 1a /62 and 1b are equivalent to each other.

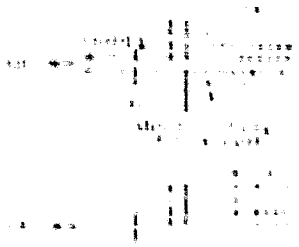

Figure 1. Idealized pull-out model

If a fiber is pulled out impulsively at one end, the load propagates through the fiber as a stress wave and reaches a discontinuous junction. For static loading, one can analyze forces acting on a fiber-matrix interface and stress variations within the fiber only by examining balance of forces without considering the inertia of a material. However, for dynamical loading, where stress waves propagate, one has to consider balance of forces taking into account the inertia of the material, that is, equations of motion. For simplicity, let us assume that layers are flat and two-dimensionality can be ignored and consider propagation of stress waves in one dimension. From Figure 2 we see that, as a pull-out stress wave reaches a discontinuous junction, equations of motion are written as

$$\rho^{(1)} \frac{\partial^2 u^{(1)}}{\partial t^2} = E^{(1)} \frac{\partial^2 u^{(1)}}{\partial x^2} \qquad (1)$$

$$\rho^{(2)} \frac{\partial^2 u^{(2)}}{\partial t^2} = E^{(2)} \frac{\partial^2 u^{(2)}}{\partial x^2} \qquad (2)$$

Figure 2. Components of forces

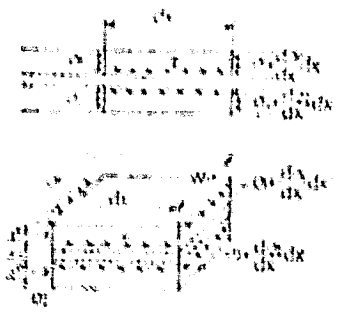

where u, E and ρ are the displacement, Young's modulo and the density for each material, respectively, while the suffix 1 or 2 corresponds to the material 1 or 2. Also $A^{(1)}$ and $A^{(2)}$ are

cross sections of materials, given respectively by

$$A^{(1)} = \pi L^{(1)}, \quad A^{(2)} = \pi L^{(2)}$$

G stands for the stiffness (shear elasticity) of a shear layer.

3. Numerical analysis

It is extremely difficult to solve Equations (1) and (2) analytically. They have been solved only under limited boundary conditions [5]. It seems almost impossible to obtain an analytical solution for the pull-out phenomenon, since the boundary condition at discontinuity is complex. Therefore, in order to obtain a realistic solution we analyzed equations numerically. Although any of the differential methods, the method of characteristic curves or the finite element method based on the Hamilton principle, may be applicable to this problem, we have employed the finite element method.

According to the Hamilton's principle, Equations (1) and (2) are equivalent to a functional Hamiltonian given by

$$H = \int_{t_1}^{t_2} \int_{x_1}^{x_2} \left[\frac{1}{2} A^{(1)} \rho^{(1)} \left(\frac{\partial u^{(1)}}{\partial t} \right)^2 + \frac{1}{2} A^{(2)} \rho^{(2)} \left(\frac{\partial u^{(2)}}{\partial t} \right)^2 \right.$$
$$- \frac{1}{2} A^{(1)} E^{(1)} \left(\frac{\partial u^{(1)}}{\partial x} \right)^2 - \frac{1}{2} A^{(2)} E^{(2)} \left(\frac{\partial u^{(2)}}{\partial x} \right)^2$$
$$\left. - \frac{1}{2} \frac{\pi G}{\ln \frac{r_2}{r_1}} \left(u^{(2)} - u^{(1)} \right)^2 \right] dx\, dt \qquad (3)$$

As shown in Figure 3, the triple layer junction of fiber-shear layer-matrix is meshed into finite number of elements. Let us denote two nodal points of the i-th element as i and i+1 and write its length as L. Displacements of the point i at time t for both materials 1 and 2 are written as

$$u_i^{(1)} \quad u^{(1)}(0, t), \quad u_{i+1}^{(2)} \quad u^{(2)}(L, t) \qquad (4)$$

Figure 3. Finite element mesh

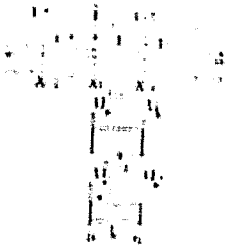

For displacements of the point i+1, one writes

$$u_{i+1}^{(n)} = u^{(n)}(L_i, t),\quad u_{i+1}^{(n+1)} = u^{(n+1)}(L_i, t) \tag{5}$$

Assuming linear variations of displacements within an element and interpolating by a linear equation of the two nodal points' displacements, one may obtain displacements within the i-th element as

$$u^{(n)} = \frac{L_i - x}{L_i} u_i^{(n)} + \frac{x}{L_i} u_{i+1}^{(n)} \tag{6}$$

$$u^{(n+1)} = \frac{L_i - x}{L_i} u_i^{(n+1)} + \frac{x}{L_i} u_{i+1}^{(n+1)} \tag{7}$$

Substitute Equations (6) and (7) into Equation (3). Take variations and set $\delta\Pi = 0$. By adding an external force on the nodal points, one gets the equation of motion for the element

$$[m]\frac{d^2}{dt^2}\{u\} + [k]\{u\} = \{f\} \tag{8}$$

where $\{u\}$ and $\{f\}$ are the nodal point displacement vector and an external force vector at the point, respectively. Their companies are given by

$$\{u\}^T = [u_i^{(n)}, u_i^{(n+1)}, u_{i+1}^{(n)}, u_{i+1}^{(n+1)}] \tag{9}$$

$$\{f\}^T = [f_i^{(n)}, f_i^{(n+1)}, f_{i+1}^{(n)}, f_{i+1}^{(n+1)}] \tag{10}$$

An element mass matrix [m] and the stiffness matrix [k] are given respectively by

$$[m] = \frac{L_i}{6}\begin{bmatrix} 2\rho^{(n)} & 0 & \rho^{(n)} & 0 \\ 0 & 2\rho^{(n+1)} & 0 & \rho^{(n+1)} \\ \rho^{(n)} & 0 & 2\rho^{(n)} & 0 \\ 0 & \rho^{(n+1)} & 0 & 2\rho^{(n+1)} \end{bmatrix} \tag{11}$$

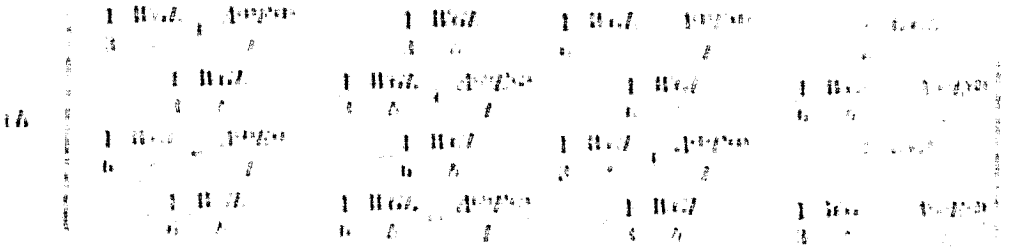

(12)

These are called a consistent mass matrix and a consistent stiffness matrix. Instead one may use lumped matrices for simplicity. They are given by

(13)

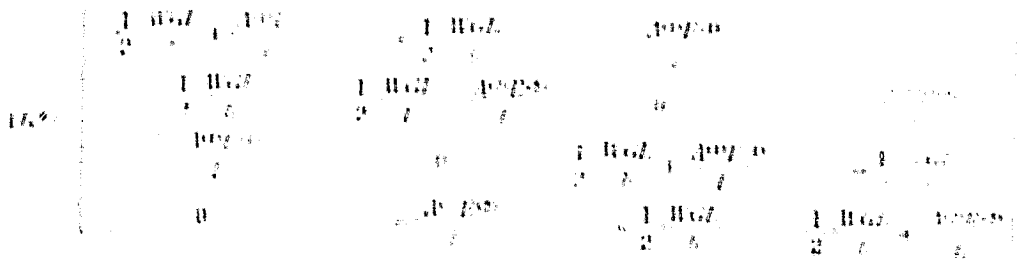

(14)

4. Experiments

We have experimented with the impulsive pull-out phenomenon using pull-out test specimens. Results will be later compared with those from numerical analysis by the finite element method.

4.1. Test specimens

Figure 4 shows the shape and the size of a test specimen as well as locations of strain gauges attached to it. A shear layer is formed by epoxy-adhesives. To investigate the effect due to the thickness of a shear layer, we used two kinds of test specimens, one with a 0.05 mm thick shear layer and another with 1 mm thickness. Both materials 1 and 2 are made of aluminum. We used commercially available epoxy-glues (Araldite) as adhesives.

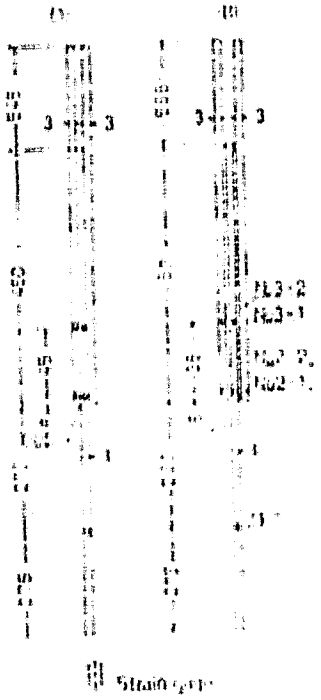

Figure 4. Test specimens

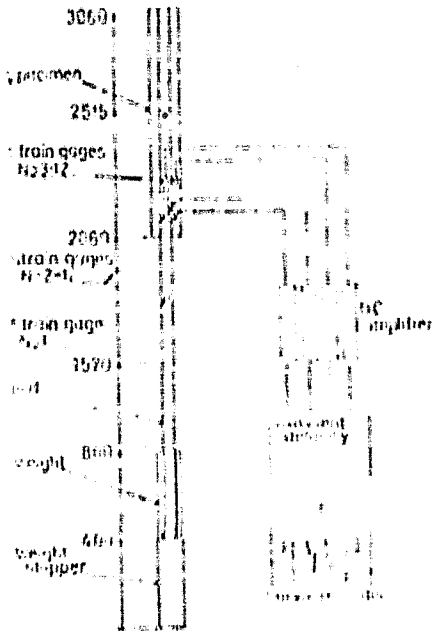

Figure 5. Experimental apparatus

4.2. Experimental apparatus

Figure 5 shows the apparatus of our experiments. Let a weight free-fall from the height of 700 mm and collide with a stopper. The collision generates stress in the rod until the weight leaves the stopper. The stress then propagates as a stress wave towards a test specimen check. When the stress wave reaches the check, a part of it is transmitted into the Material 1, while the rest propagates back inside the rod as a reflected stress wave. The transmitted wave inside the Material 1 later arrives at the adhesive junction with Material 2, and the phenomenon of an impulsive pull-out takes place. Though the shear stress at the interface between a fiber and the matrix is a crucial factor in the phenomenon of pull-out of fibers in compound materials, it is extremely difficult to measure this shear stress or shear strain. Instead, we have measured for simplicity

time variations of longitudinal strains for Materials 1 and 2 using accurate strain gauges and compared with numerical results. Signals from strain gauges were amplified by a DC-amplifier (Shinko DA-4007F; Frequency quality 50kHz/±3 db) and then recorded in digital memories. Strain gauges were 2 mm long (Kyowa KFC-2-11).

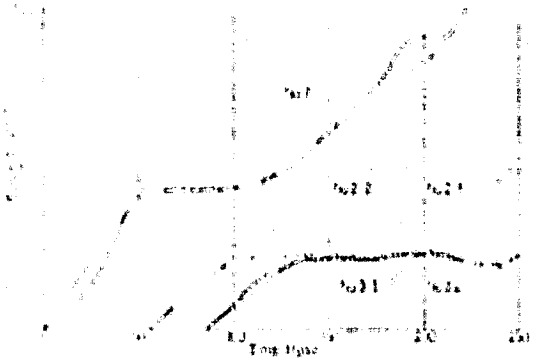

Figure 6. Stress wave records of A specimen

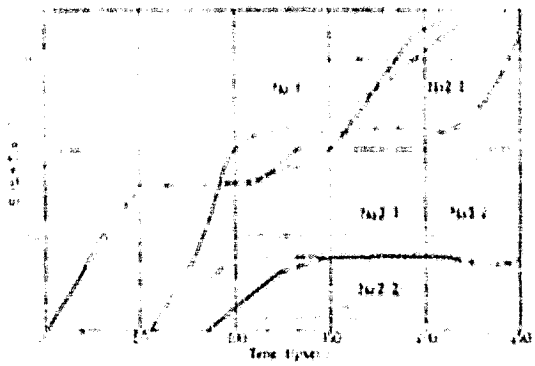

Figure 7. Stress wave records of B specimen

5. Results and discussions

5.1. Experimental results

Figures 6 and 7 show time variation of strains at each gauge location in test specimens A and B measured in the impulsive pull-out test. Here time is set at t = 0 when the front of a stress wave σ_1 in the Material 1 reaches the gauge number 1. σ_1 remains constant (with a constant stress magnitude) only during the first interval (or about 160 μsec) when the stress wave goes and returns between two ends of the stopper. Then the stress wave is transmitted and reflected multiply at both ends of the stopper and σ_1 starts to behave in a complex pattern. σ_1 is an almost step-like stress wave if the collision between a weight and a stopper is perfect, as both of them have homogeneous cross sections normal to the longitudinal direction. However, as is shown in Figures 6 and 7, σ_1 does not rise sharply as step-like, indicating an imperfect collision. The pulse is actually a ramp type with a pulse rise time of about 50 μsec. Furthermore, as is obvious in Figure 4, it is only until about 100 μsec counting from the wave front of σ_1 when only σ_1 is observed at the location of a gauge number 1. After this interval, σ_1 will be superimposed with its reflection at an predict the pattern of σ_1 any longer. Even if σ_1 is constant in time, the output from the No. 1 gauge will vary. Indeed as recorded in Fig. 6 and 7, the strain signal from the No. 1 gauge increased after 100 μ sec. This increase must be due to the superimposition of reflected waves from the adhesive junction. From the rate of increase , one may infer that σ_1 remains roughly constant until 160 sec. If the shear layer has zero thickness or its stiffness G is infinite, and the

compound material is assumed as a uniformly structured single body, variations of stress waves may be treated by the theory of elasticity stress wave propagation in one dimension [6]. For our experimental specimen σ_T (transmitted stress wave) = ½ σ_1. σ_R (reflected stress wave) = ½ σ_1. Dot-dash lines in Figures 6 and 7 are for predictions obtained from the one-dimensional wave propagation theory, assuming a uniform structure for the adhesive junction. In this computation, the incoming stress wave is taken to be a ramp type pulse with a rise time of 50 μsec. By comparing theoretical results in one dimensional wave theory with experimental results, one finds that results from the specimen A with a very thin adhesive layer agree well with theoretical predictions.

From comparison of two types of specimens A and B, one recognizes the significant difference in values of no.2-2. While the strain observed in an A specimen is consistent with that of one dimensional theory, it hardly propagates in a B specimen that has a thick shear layer. Apparently, the difference is attributed to the thickness of shear layers. The magnitude of the shear stress transmitted to the Material 2 from the Material 1 is inversely proportional to the thickness b. For small b, the transmitted shear stress is large, and two materials separated by an adhesive layer form nearly uniform single body structure. Even though the A specimen hints the similar tendency, we found that the strain measured at No.2-1 in the material, particularly in the B specimen, is larger than not only the theoretical prediction, but the incoming stress wave itself. If the shear layer is thinner and the whole adhesive junction can be regarded as a single body, then wave reflection takes place at the discontinuity where cross section changes and the wave magnitude passing through no.2-1 have to be smaller than the incoming wave. However, experimentally the strain at No.2-1 is larger than the incoming wave. For the thick shear layer the shear stress acting on the layer is small. It is not transmitted to the material immediately, even after it

propagates through the Material 1 and reaches the adhesive junctions. While the incoming stress wave stays in the Material 1 inside of the junction, it transmits the stress to Material 2. When the force is transmitted to Material 2 via shear stress, Material 1 also receives its reaction and the gauge no. 2-1 installed deeply in the junction records the strain (stress) larger than not only theoretical predicted σ_T transmitted wave, but the incoming stress wave σ_I itself. That is to say, the reflection plane for stress waves shifts effectively inward. If the shear layer gets thicker, the effective reflection plane moves further inward. Accordingly, an incoming wave penetrates into Material 1 inside of the junction and then is superimposed with its reflections. Then it is within an adhesive junction where the first large stress acts on Material 1. If Material 1 breaks down a little more than the incoming stress, then the shear breakdown of fibers could happen inside of this junction. At any rate, the one-dimensional theory may be sufficient to describe the stress far from the layer within the junction. But it fails to explain the details, much less the shear stress acting on a shear layer, that could be examined only by numerical analysis.

5.2 Numerical analysis results

As is clear from Figures 6 and 7, the stress caused by the impulse of a fallen weight in a pull-out material (fiber) may be approximated in terms of a ramp type pulse with a pulse rise time of 50 μsec. Therefore, we have examined in numerical analysis two types of loadings, one with a ramp type pulse of 50 μsec, and another with an extremely sharp step pulse. We used the /66 following parameters:

Young's modulus (for Al)	$E = 7000$ (kg/mm^2)
Density (for Al)	$\gamma = 2.75$ (g/cm^3)
Gravity acceleration	$g = 9.8$ (m/s^2)
Shear elasticity (for Araldite)	$G = 50$ (kg/mm^2)

We assumed a lumped mass matrix of Equation (13) and a consistent stiffness matrix, Equation (12). Runge-Kutta-Gill numerical method was employed to integrate equations of motion, Equation (8), while a unit interval for time integration is taken to be about 1/5 of the time required for the stress to pass through a finite element. Taking into consideration the phenomenon of wave propagation, we have divided the model in the figure into finite elements uniformly. We have used a computer HITAC 8300 (with memory capacity of 145 kb).

5.2.1 Ramp type pulse

In order to make a valid comparison with experiments, computation was done for the model in Figure 8a, which approximates the actual experimental specimen. Stress of a ramp type pulse with a rise time T = 50 μsec is assumed to act on the pull-out side of the model. The magnitude of the stress is taken to be 0.5 kg/mm^2. The length of an element is 2 mm for this computation. We analyzed the pull-out phenomenon as variations of strain at various sites in the model, until the reflected wave arrives there either from the loading end or from another free-end.

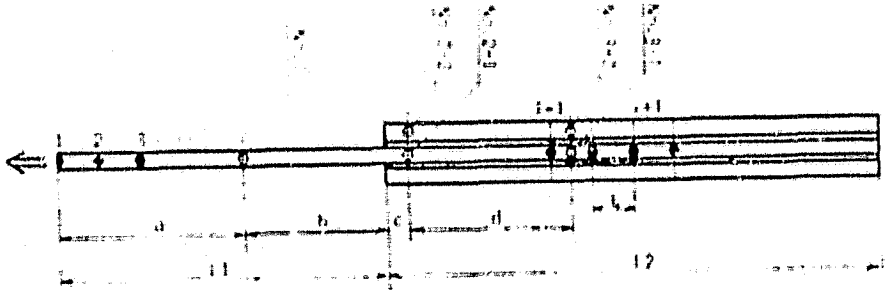

	1	11	12				
A		650	650	250	250	1	150
B	1	160	250	80	80	0.5	150

Figure 8. Finite element model for calculation

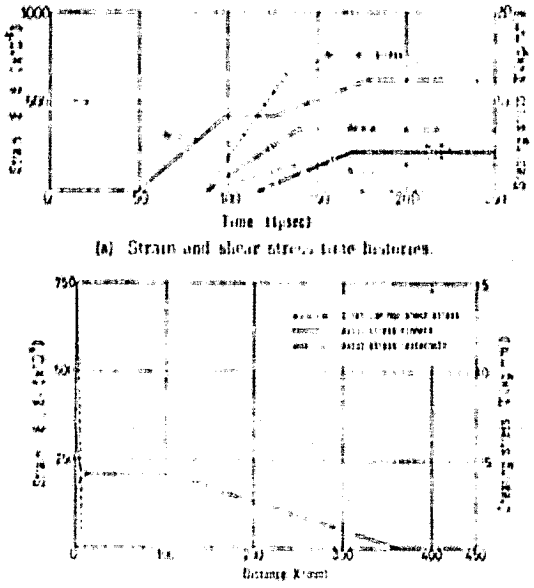

Figure 9. Calculated results of strains and shear stress in shear layer for A specimen: In case of ramp type pulse.

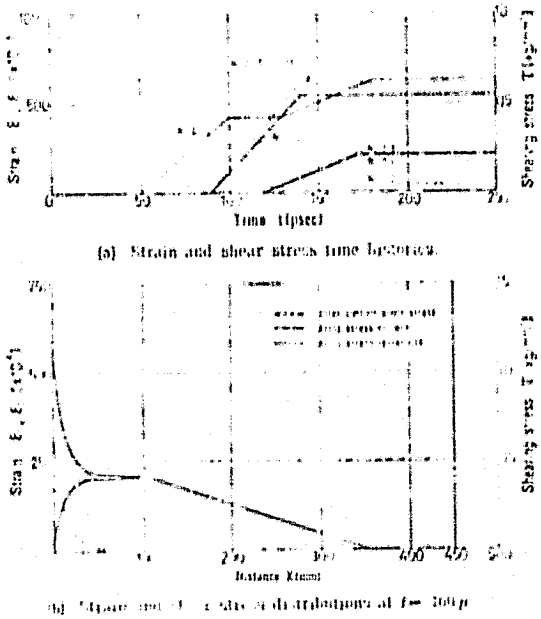

Figure 10. Calculated results of strains and shear stress in shear layer for B specimen: In case of ramp type pulse.

Results are shown in Figures 9 and 10 for the shear layer thickness b = 0.05 mm and b = 1 mm, respectively. The time t is clocked from the instance the load is applied impulsively at the loading end. From the numerical curves agreement is remarkable qualitatively as well as quantitatively with experiments, except for the gauge No. 2-1 for the shear layer of b = 0.05mm. It could explain even smaller patterns at No.2-2, that is, the effect of a shear deformation layer which could not be understood in one-dimensional stress wave propagation theory with aforementioned single body hypothesis. The largest shear stress exists at the pull-out end, regardless of the shear layer thickness. For a pulse of a long rise time 50 μsec, the shear stress increases at the arrival of stress wave and when the stress remains constant it also stays constant equal to the one under static loading. Small fluctuations are observed only towards the end of a ramp pulse where the incoming stress wave vanishes discontinuously. These oscillations get slower for a thicker shear layer. Oscillations are more visible under a step pulse loading, as will be discussed below.

5.2.2 Step pulse

The most interesting phenomenon of the impulsive pull-out is found under a step pulse loading where an incoming stress is applied more abruptly than the ramp type pulse in order to approximate a literally impulsive loading. Numerical analysis was made for the case where an incoming step pulse is realized with an extremely quick rise time T = 1 μsec on one end of the pull-out material (fiber). The model used in the analysis is shown in Figure 8b. To obtain an approximate solution for wave quations Equations (1) and (2) for a sharply rising pulse, using the finite element method one has to solve an equivalent oscillatory equation, Equation (14), where all the masses of waves with infinite number of degrees of freedom are concentrated on every nodal point that counts finite. For a better approximation, for a sharper pulse one has to use as fine a division for

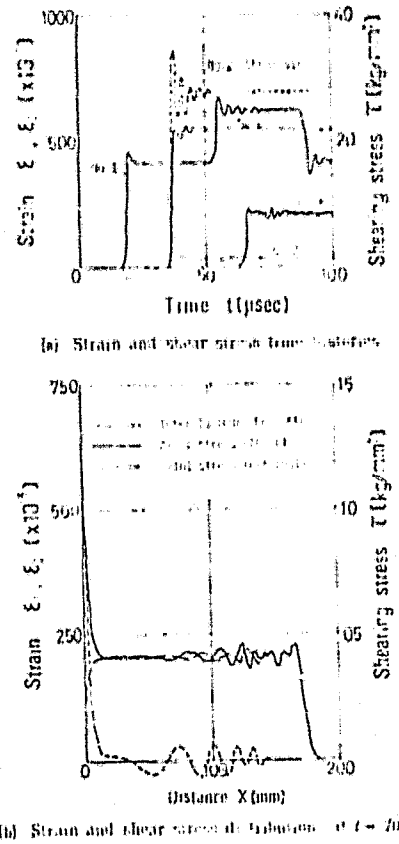

Figure 11. Calcualted results of strains and shear stress in shear layer for A specimen: in case of step pulse.

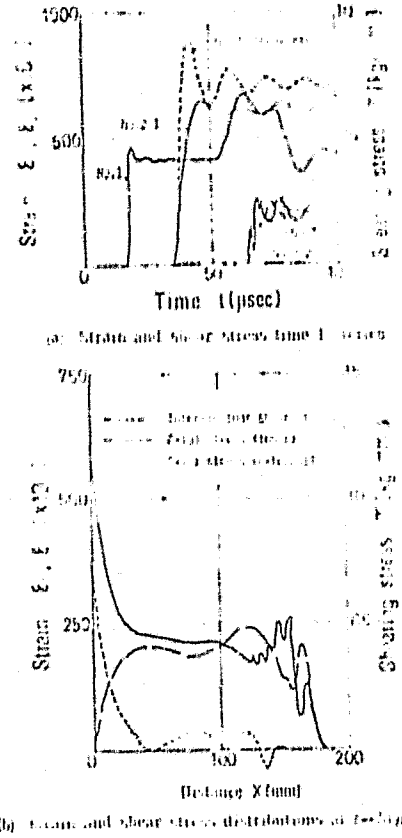

Figure 12. Calculated results of strains and shear stress in shear layer for B specimen: in case of step pulse.

each element as possible. We solved the set of differential equations numerically using the Runge-Kutta-Gill method. From consideration of the computer memory capacity and in order to minimize the number of elements to avoid a large accumulation of errors in the numerical method, we took the element length of L = 1 mm. Thus, one can examine only a short time interval in the pull-out phenomenon, yet this interval is long enough to understand the transitional phenomenon. Figure 11 shows numerical results for a b = 0.05 mm thick shear layer. One may notice a few over chutes at the top of the strain wave at the no. 1 cite sensitive to an incoming stress wave. These may be unavoidable errors in the finite element method for wave equations. Although they cannot be ignored for a detailed study, they are negligible for an understanding of a global picture of the pull-out phenomenon. The inter-laminar shear stress fluctuates in time. The fluctuation is much less visible in response to a ramp type pulse. The fluctuation in inter-laminar shear stress finally decays to the value under static loading. On the other hand, the impulsive /67 pull-out shear stress reaches a 20% larger value over the static case in a transitional response period. Also, the stress variation along a fiber is more complex. One may assume that the fluctuation of the shear stress is generated in the adhesive junction in the following mechanism. Firstly, an injected stress wave propagating in a fiber transmits the force towards the outer material, and pulls it abruptly through the shear layer, but the outer material cannot respond to it due to its inertia and then the shear stress increases. Within a fiber, particles move along the pulled direction first, but then they are decelerated. Nextly, the outer material starts being pulled, the relative displacement between the material and the fiber gets smaller and the shear stress also decreases. Particles in the outer material, by inertia, keep moving in the pulled direction, and the shear stress reduces further. Then the decrease of the stress forces the particle deceleration that is caused by the strong shear stress decrease. Consequently, the shear stress increases again in the shear layer. This whole cycle repeats many times and there is a

fluctuation of the inter-laminar shear stress. Therefore, the fluctuation must depend on the thickness of a shear layer. As is seen in Figure 12, it is less frequent for a 1 mm thick shear layer. This frequency is quite insensitive to an element length as long as the variation of the division size for finite elements is sufficiently less frequent. This insensitivity could be characteristic of the impulsive pull-out phenomenon.

6. Conclusion

Numerical analysis and experimental results are presented on the pull-out phenomenon in fiber-enforced composite materials at the high rate of loading accompanying impulsive breakdowns. The finite element method was used assuming an inter-laminar shear layer as the interface between a fiber and the matrix. If the fiber is pulled out impulsively, the shear stress is time dependent and decays into the value under static loading. Under step pulse loading, the inter-laminar shear stress fluctuates, finally decaying into the static value. The maximum shear stress under the impulsive loading assumes a value more than 20% larger than the static value.

(A lecture given at the 5th Symposium on FRP by the Japan Society of Material Science, May 31, 1979).

REFERENCES

1) S. Shimamura, Enforced Plastics 18, 410, 1972.
2) Broutman, L. J. and A. Rotem. AFOSR 72 2214 (AI) (illegible) (1972).
3) Outwater, J. O. and W.O. Carnes. Proceedings of the Army Symposium on Solid Mechanics, p. 17 (1968).
4) Lawrence, P. J. of Material Science, 7, 4 (1972).
5) Payton, R. G., J. of Applied Mech., 87, 643 (1965).
6) Timoshenko, B. P. and I. N. Goodier. Theory of Elasticity, Chap. 11 (1970) McGraw Hill Kogakusha, Md.